



# A polyacetylene derivative with pendant TEMPO group as cathode material for rechargeable batteries



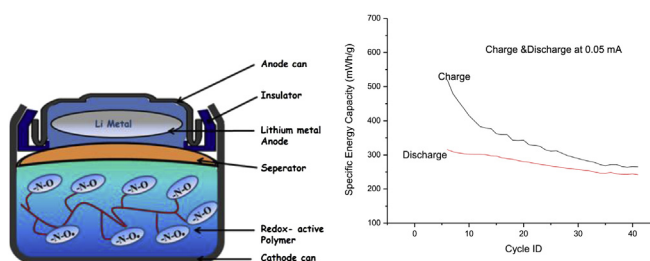
Sumeyye Bahceci<sup>1</sup>, Burak Esat\*

Fatih University, Department of Chemistry, Büyükcemce, 34500 Istanbul, Turkey

## HIGHLIGHTS

- A polyacetylene with pendant TEMPO radical has been used as a cathode active material.
- Graphite-polymer composite material cathode and Li anode have been used.
- The initial specific discharge capacity of the battery is 102.6 mAh g<sup>-1</sup>.
- The initial specific energy capacity of the battery is 315.9 mWh g<sup>-1</sup>.
- Battery has retained 77% of its energy capacity after 40 charge–discharge cycles.

## GRAPHICAL ABSTRACT



## ARTICLE INFO

### Article history:

Received 5 January 2013  
Received in revised form  
22 April 2013  
Accepted 13 May 2013  
Available online 23 May 2013

### Keywords:

Polyacetylene  
TEMPO  
Composite  
Polymer  
Cathode  
Rechargeable battery

## ABSTRACT

A composite cathode material comprised of a polyacetylene derivative with pendant TEMPO electro-active groups and graphite has been obtained and successfully utilized in a rechargeable battery against a Li anode. The battery has an initial specific discharge capacity of 102.6 mAh/g and an initial specific energy capacity of 315.9 mWh/g. This specific energy capacity is very high compared to today's conventional lithium-ion batteries with cathodes made of LiFePO<sub>4</sub>, LiCoO<sub>2</sub>, LiMnO<sub>2</sub>, etc. The battery has retained 77% of its energy capacity after 40 charge–discharge cycles.

© 2013 Elsevier B.V. All rights reserved.

## 1. Introduction

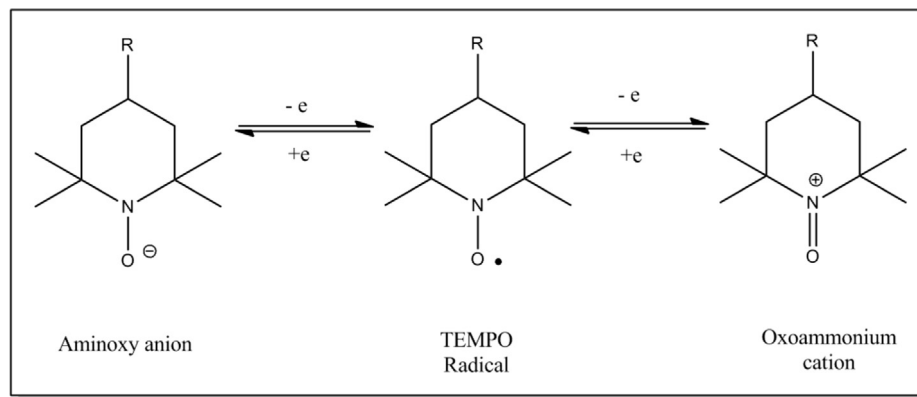
There is an increasing demand for the development of new and improved rechargeable battery technology in conjunction with today's increasing market demand in portable devices and electric

automobiles. In most of the new applications, batteries need to be lighter in weight, to be capable of fast charging, and even to be flexible in addition to having high charge and energy capacities. Most of these characteristics cannot be provided simultaneously by today's conventional rechargeable battery technology which rely on metal based electrodes. The stringent requirements such as moisture and oxygen-free environments, as well as high temperatures required for production of electrode materials make battery production difficult and costly. Polymeric materials offer many advantages over metal based materials such as their ease of

\* Corresponding author. Tel.: +90 212 866 33 00; fax: +90 212 866 34 02.

E-mail addresses: [sbahceci@fatih.edu.tr](mailto:sbahceci@fatih.edu.tr) (S. Bahceci), [besat@fatih.edu.tr](mailto:besat@fatih.edu.tr), [b\\_esat@hotmail.com](mailto:b_esat@hotmail.com) (B. Esat).

<sup>1</sup> Tel.: +90 212 866 33 00; fax: +90 212 866 34 02.



**Scheme 1.** The two redox couples of TEMPO radical.

production, processibility and tunability of their properties by chemical modification of monomer structures. The concepts of polymer electrodes and polymer batteries have attracted considerable attention after the pioneering discovery of Shirakawa that conjugated polyacetylene (PA) can become conductive when doped [1]. Conducting polymers such as polyacetylene, polythiophene and polyaniline have been investigated as potential electrode materials [2]. Their use in rechargeable batteries has been hampered because they exhibit low doping levels (leading to lower capacities) and slow electrode kinetics (which limit their charge–discharge rates). As an alternative, redox polymers with pendant electro-active functional groups which can be reversibly oxidized or reduced may be used as electrode materials. Here, the redox centers, not the polymer backbone, govern the redox behavior. However, in conjugated polymers with optional groups (substituents) attached to their backbone the spectrum of redox states offered by the polymer chain may merely be modified. Ferrocene (Fc) [6–8], carbazole groups (Cz) [9,10], tetrathiafulvalene (TTF) [3], triphenylamine (TPA) [11,12], polyoxyphenazine, and the adduct-forming polyamides and polyvinyl polymers are the general types of redox polymers. Conductivity arises when these centers can exchange charge, e.g., on account of mixed valency [3–5]. A different example of redox active functional groups is the nitroxide radical. Among nitroxides, TEMPO (2,2,6,6-tetramethylpiperidine-1-oxyl) is known to be a very robust radical and therefore has been chosen as the first electro-active pendant functional group to be used in redox polymers. TEMPO radical has two redox couples, as shown in Scheme 1, which makes it even more attractive since this gives it a propensity to be used both as an n-type (anode) material and as a p-type (cathode) material. The first attempt on the use of an organic radical as an electrode-active group for charge storage in a lithium battery was made by Nakahara's group in 2002 [13]. Polymers with pendant nitroxide radicals have been successfully utilized as cathode materials recently [14–17].

PA has been extensively studied and it has been used in a variety of battery types. Since PA can be both n-doped and p-doped, it can be used as the anode or cathode material [18–23]. Test cells using PA can exhibit specific charge densities in the range of 100–300 mAh/g. The specific energy for PA-based electrodes ranges from about 100 to 300 mWh/g. The open circuit voltage (OCV) of cells using PA as cathode depends on the counter ion. Cells using PA as the cathode and Li as the anode are generally expected to have an OCV between 3.5 and 3.9 V [24,25]. When both electrodes are PA in a cell and  $\text{Li}^+$  is used as the counter ion at the anode, the OCV is stable at ca. 3.5 V. However, it drops significantly to ca. 2.5 V when tetrabutylammonium ( $\text{Bu}_4\text{N}^+$ ) is used instead of  $\text{Li}^+$  as the counter ion [26–28]. Although there have been extensive studies on utilization of PA in batteries in the past, there has been a only very

limited amount of work on this subject recently, possibly due to stability issues and processing difficulties. However, there have been recently some important reports of cathode materials made of derivatives of PA with pendant nitroxide groups. Masuda and Katsumata reported synthesis of TEMPO and 2,2,5,5-tetramethyl-1-pyrrolidinyloxy (PROXYL)-carrying polyacetylenes by direct polymerization of TEMPO containing acetylenes with a rhodium-based transition metal catalyst [29–31]. These nitroxide radical containing PAs displayed reversible charge–discharge processes when cycled in a voltage range of 2.5–4.2 V, with capacities varying between 66 and 112 mAh/g (higher capacities obtained for PA with monomer units carrying more than one TEMPO radical unit or smaller sized PROXYL unit). Large majority of them showed a promising cycle life, that is, the capacity hardly deteriorated even after 100 cycles. Most of these polymers have displayed a gradual reduction in their discharge capacities as current densities withdrawn from batteries have been increased, presumably due to polarization effects.

In this study, we have demonstrated the use of a novel PA derivative with a pendant TEMPO radical group as a cathode active material in a rechargeable battery. The battery had an initial specific discharge capacity of 102.6 mAh/g and a specific energy capacity of 315.9 mAh/g when discharged at the rate of 0.3 C.

## 2. Experimental

### 2.1. Chemicals

All chemicals purchased were used as supplied without further purification unless stated otherwise. Solvents used for reactions

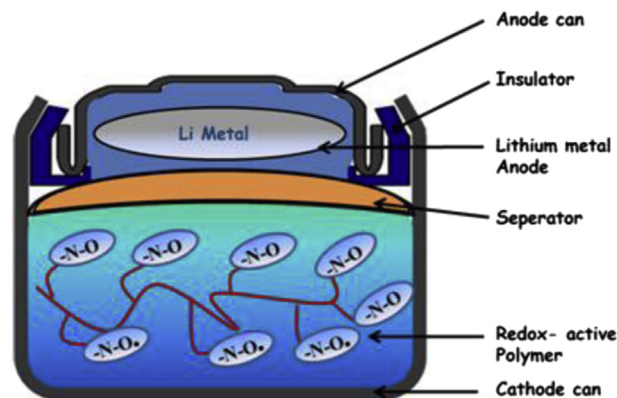
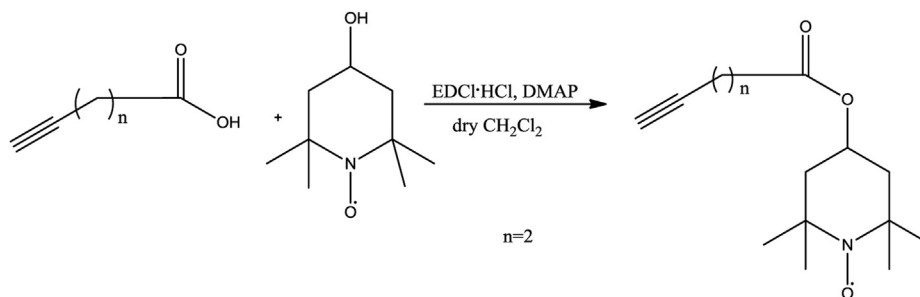


**Fig. 1.** Cell construction.



**Scheme 2.** Synthesis pathway of the monomer, 1-oxyl-2,2,6,6-tetramethylpiperidin-4-yl-pent-4'-ynoate ( $n = 2$ ).

were distilled before use according to the standard procedures. Microporous film separator (Celgard #2400) was kindly donated by Celgard Inc. The carbon conductive additive, Graphite KS6, used for the preparation of cathode composite material was donated by Timcal Ltd. Stainless Steel-CR2016 button cells cases (20 mm diameter  $\times$  1.6 mm thickness) including a circular plastic gasket were purchased from MTI Corp., U.S.A.

## 2.2. Measurements

ESR studies were performed on a BRUKER EMX series spectrometer designed for measurements in the X-band (9.5 GHz). ESR nitrogen hyperfine values were obtained via simulations using WinSim2002 program by Bruker. The polymer was characterized by the  $g$ -value (2.0065) of the ESR signal which was the same with that of TEMPO. The radical concentrations were determined by ESR spin count method, supposing that the polymers were paramagnetic at room temperature. Doubly integrated ESR nitroxide peak of the polymer under study was compared with that of the TEMPO standard.

Cyclic voltammograms were obtained with a potentiostat (CHI instrument Model 842B). Platinum disk, platinum wire, and Ag/AgCl were used as the working, auxiliary, and reference electrodes, respectively. The cyclic voltammograms were measured in an acetonitrile solution in the presence of 0.1 M tetrabutylammonium perchlorate (Bu<sub>4</sub>NClO<sub>4</sub>) as the supporting electrolyte. The polymer and graphite–polymer composite were attached to the platinum micro electrode using a silver based conducting gel. Charge/discharge properties of the coin cells prepared were measured at 25 °C using a computer controlled automatic battery analyzer (BTS-8MA/5 V/0.1–10 mA by MTI Corp.) at different charge–discharge rates.

Morphological examinations of the composite materials were determined by using a Philips XL30 SFEG scanning electron microscope (SEM).

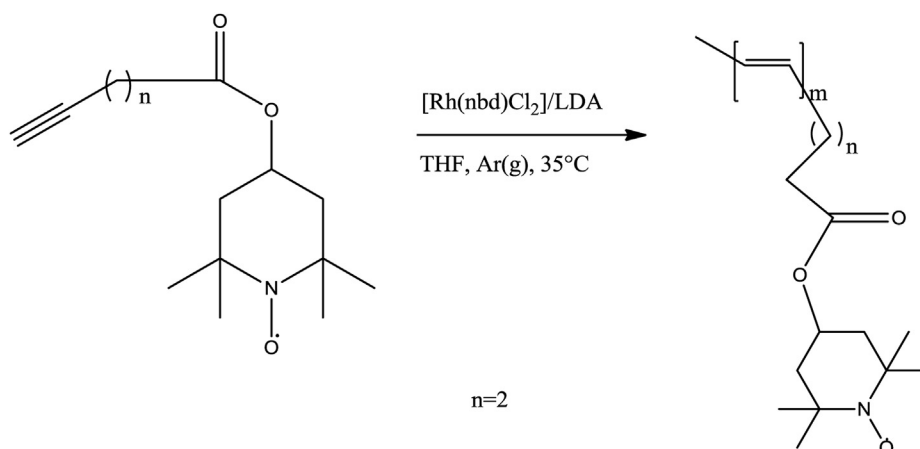
The thermal stability was determined by thermogravimetric analysis (TGA) on a STA 6000 model (Perkin Elmer Instruments). The TGA thermograms were recorded on a 5 mg of powder sample at a heating rate of 10 °C/min in the temperature range of 30–800 °C under nitrogen atmosphere.

## 2.3. Syntheses

### 2.3.1. Synthesis of monomer [1-oxyl-2,2,6,6-tetramethylpiperidin-4-yl-pent-4'-ynoate]

This monomer was synthesized according to the reported procedure [32]. 4-Pentynoic acid (500 mg, 5.097 mmol, 1.2 eq.) was added to a solution of 1-ethyl-3-(3-dimethylaminopropyl) carbodiimide hydrochloride (EDCI·HCl) and 4-dimethylamino pyridine (DMAP) (83 mg, 0.680 mmol, 0.16 eq.) in dry CH<sub>2</sub>Cl<sub>2</sub> at room temperature under N<sub>2</sub> (g). 4-Hydroxy-TEMPO (730 mg, 4.247 mmol, 1 eq.) was added to the solution, and the resulting mixture was stirred at room temperature overnight. The precipitate was filtered and the reaction mixture was washed with water (80 mL) four times, and then with brine. Finally the organic layer was dried over anhydrous MgSO<sub>4</sub>. After filtration, the solvent was removed to afford the crude product which was then purified by column chromatography (silica gel, 5:1  $\rightarrow$  7:3 hexane/ethyl acetate) to yield a dark orange solid (79% yield). M.p. 51–53.9 °C.

IR (ATR, cm<sup>-1</sup>): 3234  $\nu$ (Ar-C-H), 2997, 2974, 2932  $\nu$ (C-H), 2117  $\nu$ (C $\equiv$ C), 1726  $\nu$ (C=O), 1692, 1466, 1437, 1366  $\nu$ (N-O, radical), 1352, 1310, 1292, 1241, 1182, 1165  $\nu$ (C-O), 1091, 1051, 1003, 978, 958, 893, 710, 682. Elemental analysis: calculated for C<sub>14</sub>H<sub>22</sub>NO<sub>3</sub>: C, 66.68; H, 8.79; N, 5.55. Found: C, 65.80; H, 8.79; N, 5.46. MS  $m/z$  = 235 [M<sup>+</sup>].



**Scheme 3.** Synthesis pathway of the polymer, poly(1-oxyl-2,2,6,6-tetramethylpiperidin-4-yl-pent-4'-ynoate) ( $n = 2$ ).

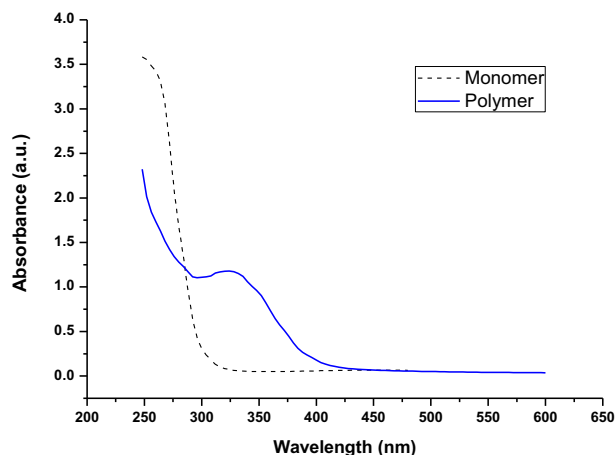


Fig. 2. UV-Vis spectra of monomer and polymer in  $\text{CHCl}_3$ .

(Theoretical  $m/z$  value = 236.16).  $^1\text{H-NMR}$  (of hydroxylamine obtained after reduction with phenylhydrazine)  $\delta_{\text{H}}$  (400 MHz,  $\text{CDCl}_3$ ): 1.8(t, 1H), 1.8–1.89, 1.5–1.55(t, 4H), 2.4(m, 4H), 5(m, 1H), 1.11, 1.13(d, 12H). ESR analysis ( $\text{CHCl}_3$  solution): three peaks at around  $g = 2.0065$  with nitrogen hyperfine value ( $A_{\text{N}}$ ) of 15.429 G (Fig. 4).

### 2.3.2. Synthesis of polymer

Polymerization was carried out using a rhodium (I) catalyst (bicyclo[2.2.1]hepta-2,5-diene-rhodium(I) chloride dimer- $[\text{Rh}(\text{nbd})\text{Cl}]_2$ ) in the presence of a cocatalyst (lithium diisopropylamide-LDA), in dry THF at 35 °C overnight. All polymerizations reactions were performed under Argon atmosphere using oven dried glassware. The typical polymerization procedure mentioned below was applied in general. A THF solution (2.38 mL) of monomer (0.3 g, 1.190 mmol) and cocatalyst LDA (0.481 mg, 4.759  $\mu\text{mol}$ ) was purged with  $\text{Ar(g)}$  and heated to 35 °C. A solution of  $[\text{Rh}(\text{nbd})\text{Cl}]_2$  (2.19 mg, 4.759  $\mu\text{mol}$ ) in THF was added with a syringe to the monomer/cocatalyst solution through a septum. The polymerization reaction was stirred overnight at 35 °C, then poured into a large amount of  $n$ -hexane or methanol to give dark or light brown polymer precipitate. The precipitate was collected by centrifuging the suspension and

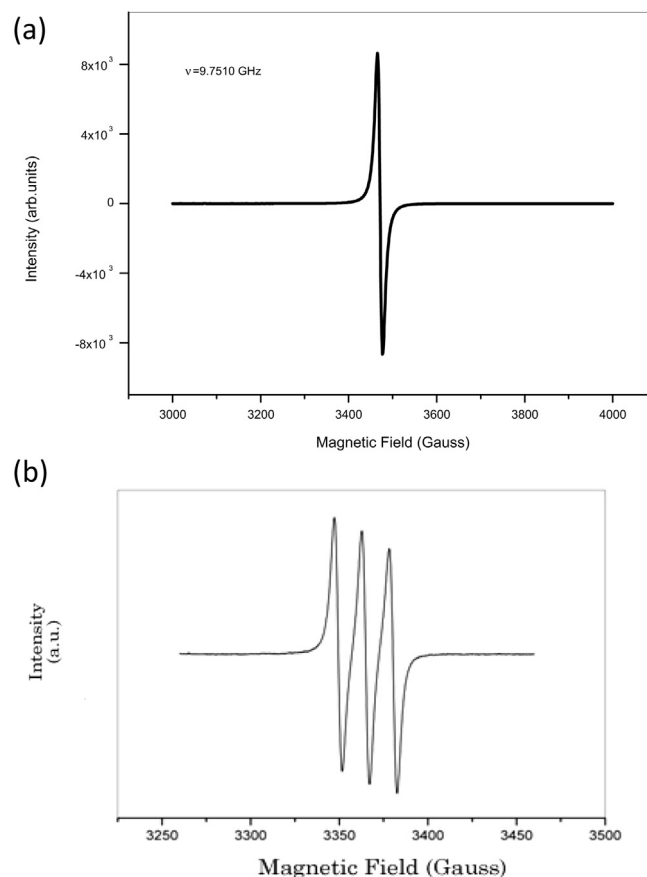


Fig. 4. ESR spectra of: (a) the polymer (powder); (b) the monomer measured (in  $\text{CHCl}_3$ ).

removal of the supernatant liquid. The precipitate was washed with hot  $n$ -hexane using a soxhlet apparatus to remove impurities such as the unreacted monomer, and then dried under vacuum to constant weight. IR (ATR,  $\text{cm}^{-1}$ ): 2974, 2937  $\nu(\text{C-H})$ , 1730  $\nu(\text{C=O, ester})$ , 1596  $\nu(\text{C=C})$ , 1463, 1363  $\nu(\text{N-O, radical})$ , 1239, 1161  $\nu(\text{C-O})$ , 1085, 983, 873, 737, 682.  $M_n = 383,700$  (THF soluble portion of polymer).

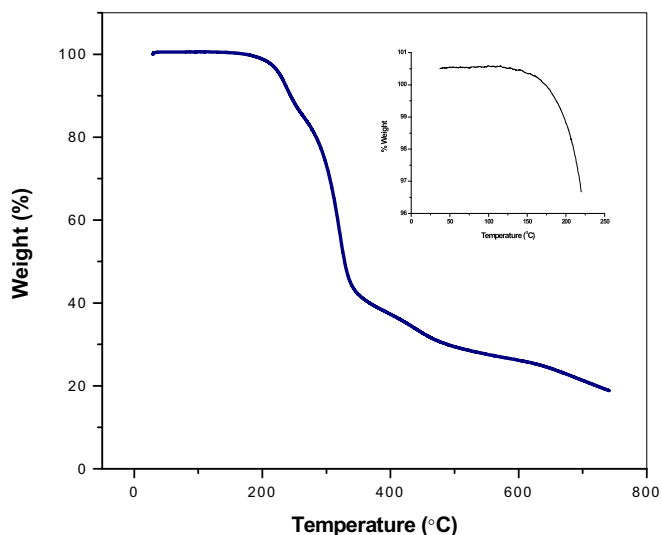


Fig. 3. TGA curve of polymer measured at heating rate of 10.0 °C/min under nitrogen flow at the rate of 20.0 ml/min. (Insert TGA curve of the polymer from RT to 220 °C).

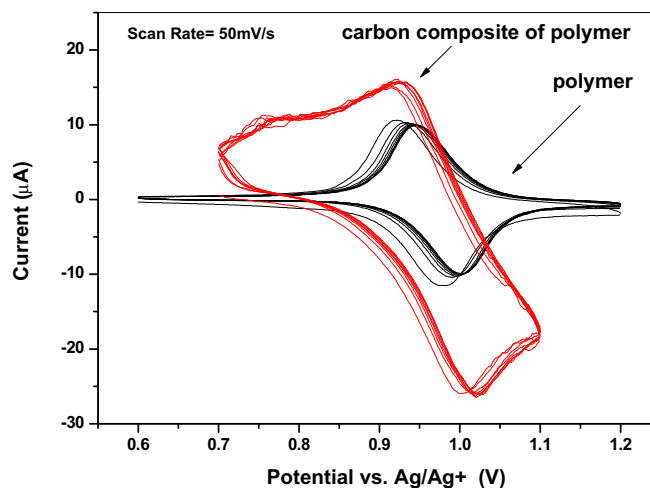


Fig. 5. The cyclic voltammetry (CV) studies of the polymer and the graphite-polymer composite



#### 2.4. Preparation of cathode composite material

The polymer (20 mg) was mixed with 70 mg of graphite conductivity agent (KS6L by Timcal) and 10 mg of a binder polymer powder (polyvinylidene fluoride resin-PVDF) in the presence of N-methyl-2-pyrrolidone (NMP). The mixture was homogenized by blending in a ball mill apparatus for an hour. Then the resulting paste was spread on aluminum foil (a circular disc 19 mm in diameter) and dried overnight in vacuum at 70 °C to obtain the electrodes. Thicknesses of these cathodes were about 0.1 mm. The mass of active polymeric material in the cathode was about 2 mg.

#### 2.5. Cell construction

A 2016 type coin cell was fabricated by stacking the polymer/graphite composite cathode, porous polypropylene separator sheet (Celgrad #2400, Hoechst Celanese Co., Ltd.), a lithium foil anode and a stainless steel current collector under dry argon atmosphere. A mixture of ethylene carbonate/diethylcarbonate (EC:DEC) (1:1 v/v) containing 1 M of  $\text{LiPF}_6$  was used as the electrolyte solution. Battery charge–discharge characteristics were evaluated by using a computer controlled battery charge–discharge instrument (Fig. 1).

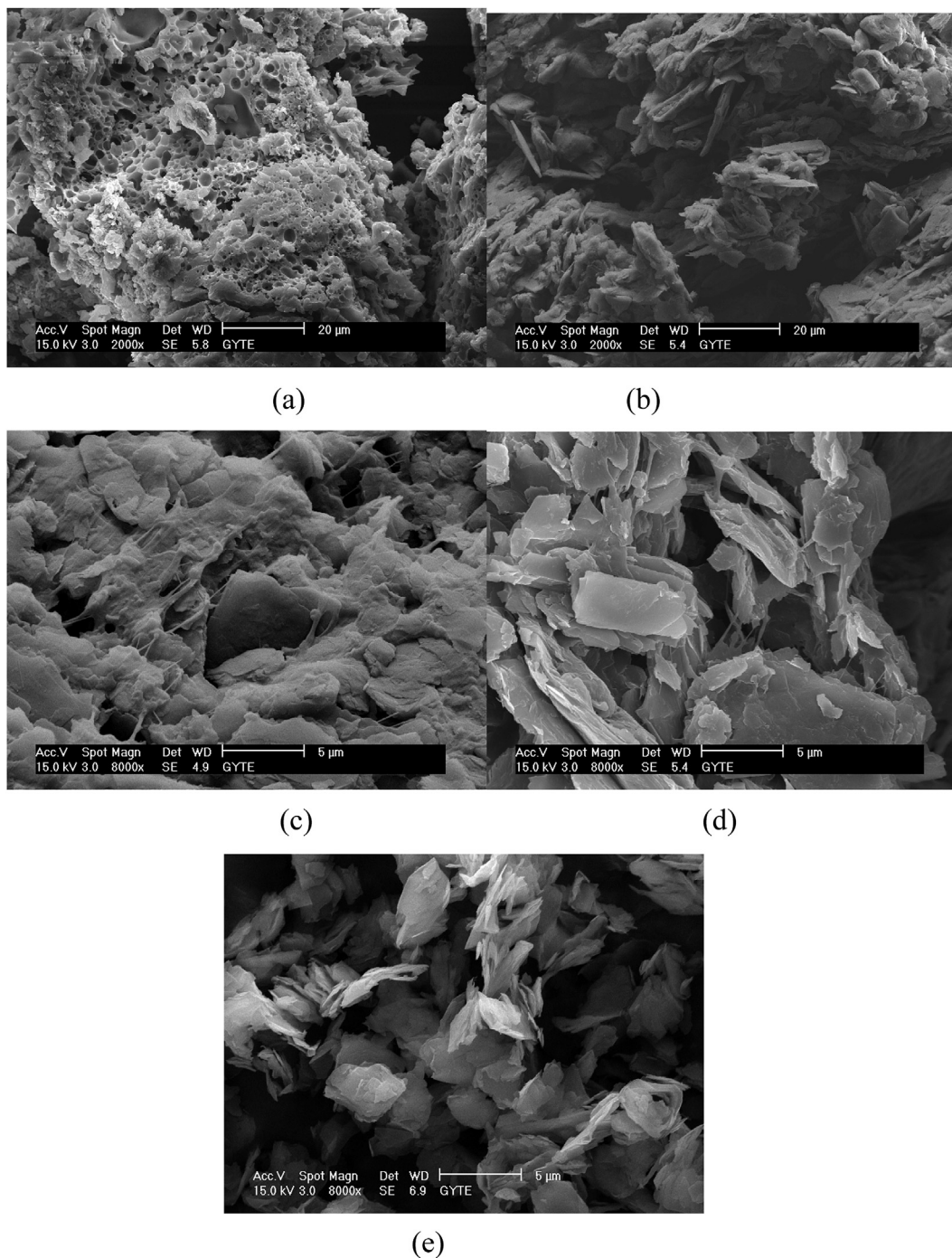


**Fig. 6.** SEM images of: polymer (a), polymer–graphite–PVDF composite (b–d), graphite (e).

### 3. Results and discussion

Acetylenic monomer, 1-oxy-2,2,6,6-tetramethylpiperidin-4-yl pent-4'-ynoate, was synthesized by the coupling of the carboxyl group of 4-pentynoic acid with the hydroxy group of 4-hydroxy TEMPO (4-hydroxy-2,2,6,6-tetramethylpiperidin-1-oxy) with a yield of 79% (Scheme 2). The structure of the monomer was confirmed by IR(ATR) and  $^1\text{H}$ -NMR spectroscopies, and by elemental and mass spectral analysis (see Section 2).

The polymerization of acetylenic monomer was carried out using  $[\text{Rh}(\text{nbd})\text{Cl}]_2$  catalyst together with LDA cocatalysts in THF at  $35^\circ\text{C}$  for overnight (Scheme 3). Polymer was obtained as a brown powder in 51% yield. The THF soluble portion of the polymer had a number average molecular weight ( $M_n$ ) of 383 700 and a polydispersity index (PDI) of 1.25. However, the THF insoluble portion which constitutes about 62% by mass of the entire polymer sample is believed to have a much higher molecular weight. The polymer was found to be completely insoluble in *n*-hexane and diethyl ether. The differences in solubility can be attributed to presence of different ratios of *cis*-transoid, all-transoid and all-cisoid configurations of neighboring double bonds in the polyacetylene backbone. Polymer aggregation also plays important role in the solubility behavior of the polymer obtained. The polymer exhibited no IR peaks at around  $3270$  and  $2120\text{ cm}^{-1}$  that arise from stretching vibrations of *sp* C–H and  $\text{C}\equiv\text{C}$  bonds respectively, thus indicating that acetylene polymerization was complete.

Fig. 2 illustrates the ultraviolet/visible (UV/Vis) spectra of the polymer obtained and the monomer in  $\text{CHCl}_3$  for comparison. The  $\text{CHCl}_3$  soluble portion of polymer displayed a broad absorption peak near visible spectral region, with absorption maxima at about  $324\text{ nm}$  extending to  $400\text{ nm}$ , which indicates the presence of a conjugated backbone in the polymer chain. The monomer, on the other hand, showed no absorption wavelength in this region.

TGA (thermal gravimetric analysis) illustrated in Fig. 3 shows that the polymer is thermally stable up to about  $200^\circ\text{C}$ . Remarkable weight losses were detected above  $200^\circ\text{C}$  as a result of thermal decompositions of the TEMPO moiety and the polymer main chain.

Fig. 4a depicts the electron spin resonance (ESR) spectrum of polymer in the solid state. The polymer exhibited a sharp singlet signal based on the TEMPO radical with *g*-value of 2.00878, which is close to that of the TEMPO crystal (*g*-value = 2.00935). ESR spectrum of monomer in  $\text{CHCl}_3$  showed a characteristic nitroxide triplet at around  $g = 2.0065$  with a nitrogen hyperfine value ( $A_N$ ) of  $15.429\text{ G}$  as given in Fig. 4b. The spin concentration of polymer was determined by ESR spin count method, supposing that the polymers are paramagnetic at room temperature. A spin concentration of  $3.522 \times 10^{21}$  spins/g of polymer which nearly corresponds to 1 spin per repeating unit was obtained.

The cyclic voltammetry (CV) studies of the polymer and the graphite–polymer composite (Fig. 5) reveals that both polymer and its composite can be reversibly oxidized. For the polymer, oxidation and reduction peaks at  $1.002\text{ V}$  and at  $0.946\text{ V}$  (vs  $\text{Ag}/\text{Ag}^+$  reference electrode) respectively were observed due to reversible redox behavior of TEMPO radical moiety. The composite material showed an oxidation peak at  $1.017\text{ V}$  and a reduction peak at  $0.923\text{ V}$ . The gap between the oxidation and reduction peaks ( $\Delta E_{\text{pp}}$ ) of the polymer and the composite material are  $0.056$  and  $0.094$ , respectively. These values are smaller compared to the  $\Delta E_{\text{pp}}$  value of the first generation TEMPO based cathode active material ( $0.146\text{ V}$ ), 2,2,6,6-tetramethylpiperidinyloxy methacrylate (PTMA) [13,33,34]. This implies that the reversible redox reaction rates of our polymer and composite material are higher than that of PTMA, and therefore rechargeable batteries utilizing our polymer are expected to have a better charge–discharge rate behavior compared to those utilizing PTMA. The larger  $\Delta E_{\text{pp}}$  value of the composite material compared to

that of pure polymer is probably caused by the use of a relatively thick composite sample during measurement, which may lead to presence of diverse electrochemical microenvironments around the nitroxide moiety in the bulk of the composite material. The

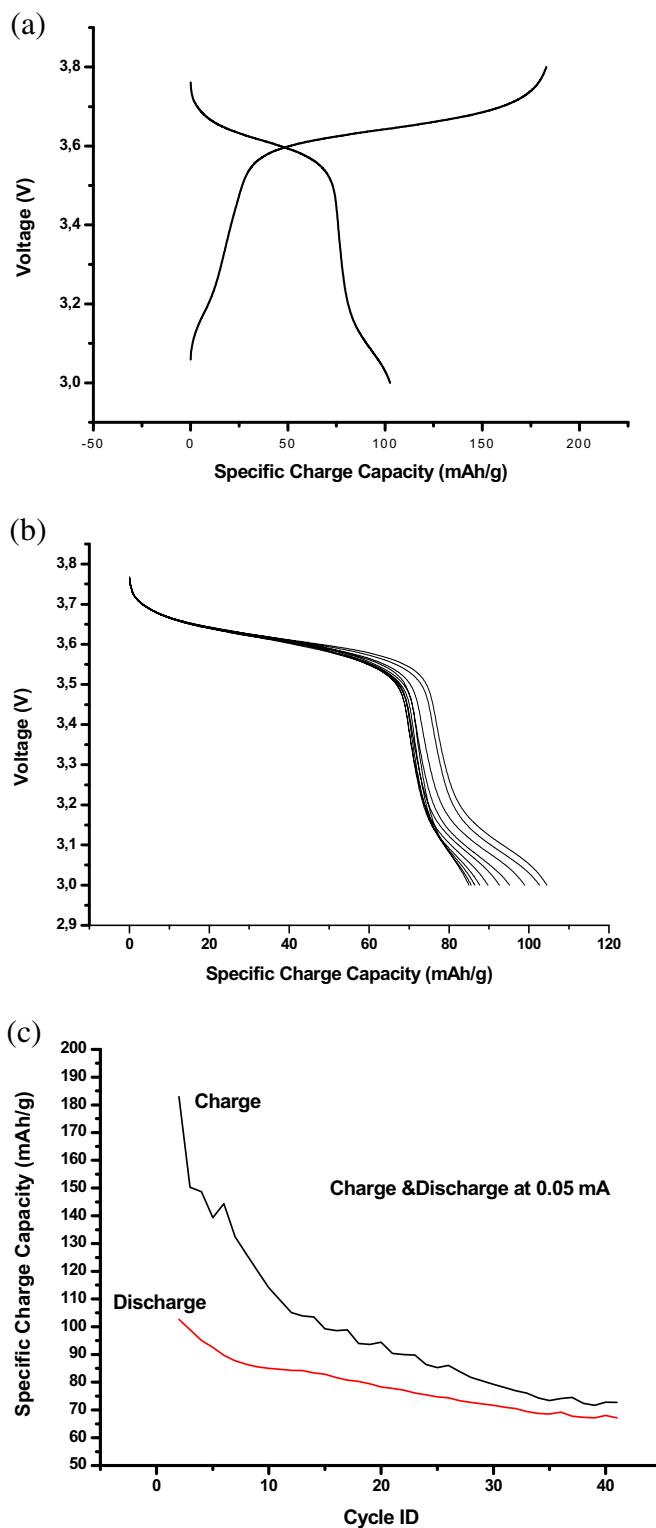


Fig. 7. (a) Voltage vs. specific charge/discharge capacity for the first cycle, (b) voltage vs. specific discharge capacity for the first 10 cycles, (c) specific charge/discharge capacity vs cycle behavior curves at the constant current charge/discharge rate of  $0.05\text{ mA}$ .

redox behaviors of the polymer and composite has scarcely changed during CV scans, indicating that they are electrochemically quite stable.

SEM pictures of polymer and polymer–graphite–PVdF (2:7:1) composite are shown in Fig. 6. SEM image analysis indicates a porous structure for the polymer (Fig. 6a). The morphology of composite is characterized by flat particles of graphite covered homogeneously by polymer as seen in Fig. 6(b)–(d). The graphite particle size appears to be quite large ( $\sim 5 \mu\text{m}$ ).

Charge–discharge properties were investigated by performing constant current charge–discharge cycles on the cell constructed. Fig. 7a shows specific charge capacities for the first charge–discharge cycle of the cell performed at the rate of 0.05 mA. At this charge/discharge rate (which charges/discharges the cell in approximately 3.5 h, therefore equals to 0.3 C rate), the initial specific charge and discharge capacities are 182.9 and 102.6 mAh/g, respectively. The discharge curves clearly depicts that the cell has discharged most of its capacity around 3.6 V vs. Li which is the characteristic redox potential of TEMPO radical. In the first cycle, the cell was able to discharge only 56% of the charge it acquired during charging (Fig. 7a). This low discharge efficiency, however, continually improved in the subsequent cycles and reached a value of 92% at the end of 40 cycles. This can be attributed to the fact that only a fraction of the positively charged oxoammonium species obtained by the oxidation of TEMPO moieties during charging could be converted back to TEMPO group (Scheme 1) during the subsequent discharging (which may be due to slow counter ion movement in the bulk of the material). This incomplete recovery of the TEMPO group also explains the reduction in cell capacity as the cycling is continued.

The specific charge and discharge capacities reached a plateau and appeared to be 72.8 and 68.0 mAh/g respectively after 40 cycles (Fig. 7c). The total discharge capacity loss after 40 cycles was observed to be 34.6 mAh/g. As can be seen in Fig. 7a, 21.5 mAh/g of the initial capacity discharged (102.6 mAh/g) was extracted from the cell in 3.0–3.2 V range. This portion of the discharge curve seemed to erode to a great extent during charge–discharge cycling (Fig. 7b) which accounted for about 62% of the total discharge capacity loss. We think that the capacity in this region may be attributed to the irreversible redox reaction of the conjugated PA backbone.

Initial specific energy capacity of the cell was measured to be 315.9 mWh/g (Fig. 8). Although it decreased to 244.7 mWh/g at the end of 40 cycles (approximately 77% of its energy capacity

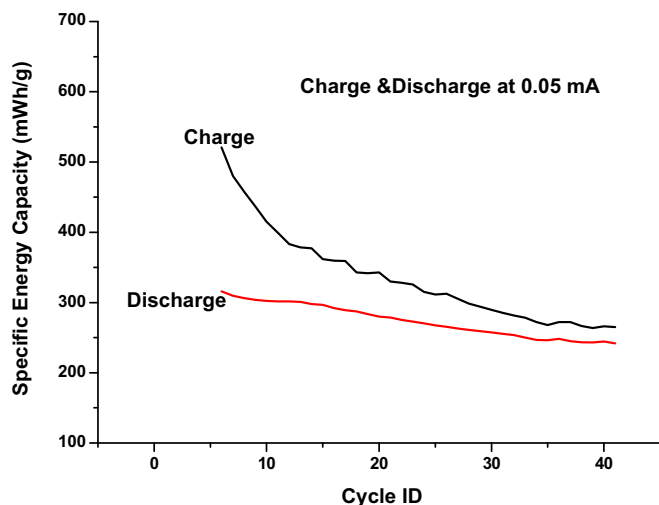


Fig. 8. Cycle behavior of specific energy capacity at 0.05 mA charge/discharge rate.

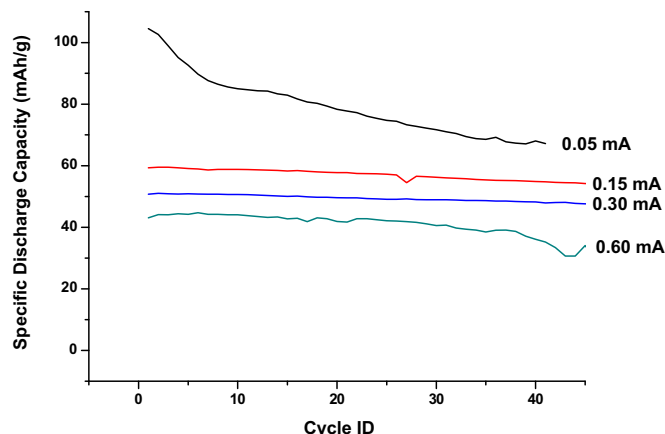


Fig. 9. Specific discharge capacity vs. cycle number at various discharge rates.

retained), it is still comparable to that of a typical commercial Li-ion battery ( $\leq 200 \text{ mWh/g}$ ). The cell was also charged and discharged at higher constant current rates. The specific discharge capacity was decreased from 68.0 to 54.8, 48.2, and 36.1 as the discharge rate increased from 0.05 mA to 0.15 mA, 0.30 mA and 0.60 mA respectively (Fig. 9). It can be seen that the specific discharge capacity remains approximately constant during charge and discharge cycles, which indicates the quite good cycling behavior of the cell even at high charge/discharge rates.

#### 4. Conclusion

Synthesis of a novel polyacetylene derivative with pendant nitroxide radical redox active group and its utilization in the form of graphite composite as a cathode in a rechargeable battery were demonstrated successfully. The cathode material obtained exhibited an initial specific energy density of 315.9 mWh/g and retained approximately 77% of this after 40 cycles at 0.3 C discharge rate. This is higher than those of today's conventional commercial rechargeable lithium-ion batteries (200 mWh/g). A total of 66.2% of the initial discharge capacity was preserved after 40 cycles. When subjected to further cycling at moderate discharge rates of 0.9 C (0.15 mA) and 1.8 C (0.30 mA) the charge capacity remained almost constant around 55 and 50 mAh/g, respectively. Although these values are lower compared to those of commercial cathode materials utilized in rechargeable Li-ion batteries (140 mAh/g for  $\text{LiCoO}_2$ , 150 mAh/g for  $\text{LiFePO}_4$ ), the results are still promising. Once the problems such as the charge capacity loss during cycling (which may be due to inefficient counter ion transport and/or electrode material dissolution) are solved, experimental charge capacity values equal to the theoretical ones are believed to be realized. Thus, there is a great potential for polymeric electro-active materials to be used in rechargeable batteries as alternatives to the conventional electrode materials. With the advent of polymeric anode materials of the suitable reduction potentials concomitant with advent of polymeric cathode materials, all-polymer, flexible, light-weight and environmentally benign batteries could be developed which may provide advantages such as revoking the requirement for humidity-free and oxygen-free environments during manufacturing. This may lead to lower manufacturing and facility set-up costs, and to new cell chemistries with improved properties.

#### Acknowledgements

This work was financially supported by Fatih University (BAP 50020801-2) and by TUBITAK (project no. 108T596).

## Appendix A. Supplementary data

Supplementary data related to this article can be found at <http://dx.doi.org/10.1016/j.jpowsour.2013.05.051>.

## References

- [1] H. Shirakawa, E.J. Louis, A.G. MacDiarmid, C.K. Chiang, E.J. Heeger, Synthesis of electrically conducting organic polymers: halogen derivatives of polyacetylene, (CH)<sub>x</sub>, *J. Chem. Soc. Chem. Commun.* (1977) 578.
- [2] P. Novak, K. Müller, K.S.V. Santhanam, O. Haas, Electrochemically active polymers for rechargeable batteries, *Chem. Rev.* 97 (1997) 207–281.
- [3] F.B. Kaufman, A.H. Schroeder, E.M. Engler, S.R. Kramer, J.Q. Chambers, Ion and electron transport in stable, electroactivetetrathiafulvalene polymer coated electrodes, *J. Am. Chem. Soc.* 102 (1980) 483.
- [4] Y. Shirota, T. Kakuta, H. Mikawa, Electrochemical oxidation of poly(vinylferrocene) with concurrent precipitation on the electrode: preparation of an electrically conducting polymer, *Makromol.Chem. Rapid Commun.* 5 (1984) 337.
- [5] C. Iwakura, T. Kawai, M. Nojima, H. Yoneyama, A new electrode-active material for polymer batteries polyvinylferrocene, *J. Electrochem. Soc.* 134 (1987) 791.
- [6] T. Suga, H. Konishi, H. Nishide, Photocrosslinkednitroxide polymer cathode-active materials for application in an organic-based paper battery, *Chem. Commun.* (2007) 1730.
- [7] H.F. Bittner, C.C. Badcock, Electrochemical utilization of metal hydrides, *J. Electrochem. Soc.* 130 (1983) 193C.
- [8] Y. Shirota, N. Noma, H. Kanega, H.J. Mikawa, Preparation of an electrically conducting polymer by the electrolytic polymerization of N-vinylcarbazole, *Chem. Soc. Chem. Commun.* (1984) 470.
- [9] T. Kakuta, Y. Shirota, H. Mikawa, A rechargeable battery using electrochemically doped poly(N-vinylcarbazole), *J. Chem. Soc. Chem. Commun.* (1985) 553.
- [10] M. Baibarac, M. Lira-Cantú, J.O. Sol, I. Baltog, N. Casañ-Pastor, P. Gomez-Romero, Poly(N-vinyl carbazole) and carbon nanotubes based composites and their application to rechargeable lithium batteries, *Compos. Sci. Technol.* 67 (2007) 2556–2563.
- [11] R.G. Compton, M.J. Day, A. Ledwith, I.I. Abu-Abdoun, The modification of electrodes with poly(4-vinyl-4',4''-dibromotriphenylamine), *J. Chem. Soc. Chem. Commun.* (1986) 328.
- [12] R.G. Compton, M.E. Laing, A. Ledwith, I.I. Abu-Abdoun, Polymer-coated electrodes: cyclic voltammetry and chronoamperometry of non-ideal systems – the anodic oxidation of poly(4-vinyl-triphenylamine) films, *J. Appl. Electrochem.* 18 (1988) 431.
- [13] K. Nakahara, S. Iwasa, M. Satoh, Y. Morioka, J. Iriyama, M. Suguro, E. Hasegawa, Rechargeable batteries with organic radical cathodes, *Chem. Phys. Lett.* 359 (2002) 351.
- [14] P. Nesvadba, L. Bugnon, P. Maire, P. Novak, Synthesis of a novel spirobisnitroxide polymer and its evaluation in an organic radical battery, *Chem. Mater.* 22 (2010) 783–788.
- [15] T. Suga, S. Sugita, H. Ohshiro, K. Oyaizu, H. Nishide, p- and n-type bipolar redox-active radical polymer: toward totally organic polymer-based rechargeable devices with variable configuration, *Adv. Mater.* 23 (2011) 751–754.
- [16] Y. Liang, Z. Tao, J. Chen, Organic electrode materials for rechargeable lithium batteries, *Adv. Energy Mater.* 2 (2012) 742–769.
- [17] T. Suga, H. Nishide, Redox-active radical polymers for a totally organic rechargeable battery, In: ACS Symposium Book Series, *Polymers for Energy Storage and Delivery: Polyelectrolytes for Batteries and Fuel Cells*, vol. 1096 2012, pp. 45–53.
- [18] D. MacInnes Jr., et al., Organic batteries: reversible n-and p-type electrochemical doping of polyacetylene (CH)<sub>x</sub>, *J. Chem. Soc. Chem. Commun.* (1981) 317.
- [19] C.K. Chiang, An all-polymeric solid state battery, *Polym. Commun.* 22 (1981) 1454.
- [20] T. Nagatomo, et al., A long-lasting polyacetylene battery with high energy density, *Jpn. J. Appl. Phys.* 22 (1983) L275.
- [21] G.C. Farrington, R. Huq, Polyacetylene electrodes for non-aqueous lithium batteries, *J. Power Sources* 14 (1985) 3.
- [22] T. Nagatomo, C. Ichikawa, O. Omoto, All-plastic batteries with polyacetylene electrodes, *J. Electrochem. Soc.* 134 (1987) 305.
- [23] O.N. Efimov, et al., Laminated composites based on polyacetylene and Al–Mg alloy negative electrode materials for Li rechargeable batteries, *Synth. Met.* 79 (1996) 193.
- [24] G.C. Farrington, et al., The electrochemical oxidation of polyacetylene and its battery applications, *J. Electrochem. Soc.* 131 (1984) 7.
- [25] J.C.W. Chien, J.B. Schlenoff, Limiting battery performance parameters for polyacetylene, *Nature* 311 (1984) 362.
- [26] A. Skotheim, J.R. Reynolds (Eds.), *Handbook of Conducting Polymers-Conjugated Polymers Processing and Applications*, third ed., CRC Press, Boca Raton, London, New York, 2007. (Chapter 9), p. 7.
- [27] R.B. Kaner, A.G. MacDiarmid, R.J. Mammone, *Polymers in electronics*, ACS Symp. Ser. 242 (1984) 575.
- [28] A.G. MacDiarmid, Polyacetylene batteries, *Prog. Batteries Sol. Cells* 5 (1984) 31.
- [29] T. Katsumada, M. Satoh, J. Wada, M. Shiotsuki, F. Sanda, T. Masuda, Polyacetylene and polynorbornene derivatives carrying TEMPO. Synthesis and properties as organic radical battery materials, *Macromol. Rapid Commun.* 27 (2006) 1206–1211.
- [30] J. Qu, T. Katsumata, M. Satoh, J. Wada, J. Igarashi, K. Mizoguchi, T. Masuda, Synthesis and charge/discharge properties of polyacetylenes carrying 2,2,6,6-tetramethyl-1-piperidinyloxy radicals, *Chem. Eur. J.* 13 (2007) 7965–7973.
- [31] J. Qu, T. Fujii, T. Katsumata, Y. Suzuki, M. Shiotsuki, F. Sanda, M. Satoh, J. Wada, T. Masuda, Helical polyacetylenes carrying 2,2,6,6-tetramethyl-1-piperidinyloxy and 2,2,5,5-tetramethyl-1-pyrrolidinyloxy moieties: their synthesis, properties, and function, *J. Polym. Science: Part A Polym. Chem.* 23 (2007) 5431–5445.
- [32] J.A. Opsteen, J.C.M. Van Hest, Modular synthesis of block copolymers via cycloaddition of terminal azide and alkyne functionalized polymers, *Chem. Commun.* (2005) 57–59.
- [33] H. Nishide, S. Iwasa, Y.J. Pu, T. Suga, K. Nakahara, M. Satoh, Organic radical battery: nitroxide polymers as a cathode-active material, *Electrochim. Acta* 50 (2004) 827–831.
- [34] M. Satoh, K. Nakahara, J. Iriyama, S. Iwasa, M. Suguro, High power organic radical battery for information systems, *IEICE Trans. Electron. (Inst. Electron Inf. Commun. Eng.)* E87–C(12) (2004) 2076–2080.